Juvotek | Jurnal Vokasi Teknik

Mentech.id

RESEARCH ARTICLE OPEN ACCESS

Effect of Shielding Gas Flow Rate on the Load-Bearing Response of GMAW-Welded Low-Carbon Steel Specimens

Manahan Hutagallung[*1], **Ricky Sanjaya**[2]

[1]Teknik Mekanika, Politeknik Teknologi Kimia Industri Medan, Indonesia.
[2]Fakultas Teknik, Universitas Muhammadiyah Sumatera Utara, Indonesia.

Received: January 09, 2024 | Accpeted: March 15, 2024 | Published: April 01, 2024

ABSTRACT

Shielding gas flow rate is an important parameter in gas metal arc welding (GMAW), but its relationship with the mechanical response of welded low-carbon steel specimens depends on the welding and testing conditions. This study investigated the effect of shielding gas flow rates of 10, 20, and 25 L/min on the maximum load recorded during compression testing. Three specimens with nominal dimensions of 100 × 40 × 4 mm and V-groove joints were welded at a nominal current of 120 A, with one specimen tested at each flow rate. The maximum recorded loads were 440 kgf at 10 L/min, 460 kgf at 20 L/min, and 460 kgf at 25 L/min. The increase from 10 to 20 L/min corresponded to a descriptive increase of approximately 4.55%, whereas increasing the flow rate from 20 to 25 L/min produced no additional recorded load benefit. These findings provide a preliminary comparison of shielding gas settings and the loading response of the investigated welded specimens. However, the absence of replicated tests prevents statistical assessment of the observed differences or identification of an optimum flow rate. Furthermore, the original area calculation requires verification before the derived values can be interpreted as compressive strength. The results identify 20 L/min as a candidate for further experimental evaluation, subject to replicated testing, validated loading geometry, and improved welding-process documentation.

Keywords:
gas metal arc welding (GMAW); shielding gas flow rate; low-carbon steel; compression testing; maximum load; welded joints.

Article Info

Check for updates

EDITED BY
Dr. Ir. Arman
Pascasarjana STIE Bangkinang, Indonesia.

COPYRIGHT©2024 (Author)
Manahan Hutagallung,
Ricky Sanjaya

***CORRESPONDENCE**
Manahan Hutagallung
manahanhutagalung019@gmail.com

This work is licensed under a Creative Commons Attribution-ShareAlike 4.0 International License.

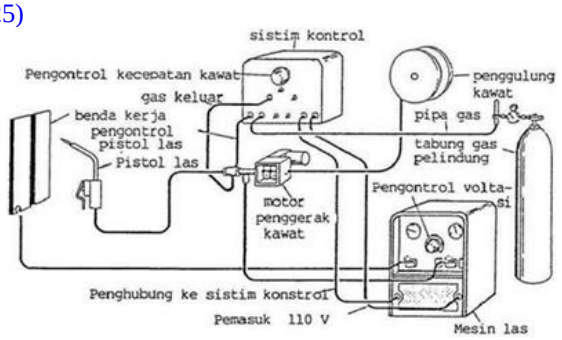
To cite this article:
Hutagalung, M., & Sanjaya, R. (2024). Effect of Shielding Gas Flow Rate on the Load-Bearing Response of GMAW-Welded Low-Carbon Steel Specimens. Jurnal Vokasi Teknik, 2(1), 26-34. https://doi.org/10.67922/76av6k27

INTRODUCTION

Research Context and Manufacturing Significance

Gas metal arc welding (GMAW) is an established joining process for manufacturing low-carbon steel components. Its continuous wire feed supports productive fabrication, while the externally supplied shielding gas protects the welding region(Liu et al., 2021, p. 1; Wordofa & Ramulu, 2023, p. 366). For manufacturers, the practical challenge is to produce joints with suitable mechanical performance while controlling process variability and consumable use. Shielding gas selection therefore involves both weld integrity and production efficiency, rather than gas delivery alone (Campbell et al., 2012; Fortain & Gadrey, 2013).

Figure 1 illustrates the principal components of the GMAW system, including the power source, wire feed mechanism, welding gun, and shielding gas supply. Within this arrangement, gas flow rate is an adjustable parameter whose effectiveness depends on the interaction between the gas stream, welding arc, and surrounding atmosphere. Understanding this interaction is necessary when selecting settings for a particular material, joint geometry, and manufacturing application (Bitharas et al., 2017; Jia et al., 2025)



Note. English label key: control system; wire feed speed control; gas outlet; workpiece; welding gun trigger; welding gun; wire feed motor; connection to control system; 110 V input; welding power source; voltage control; wire spool; gas hose; shielding gas cylinder.

Figure 1. GMAW equipment arrangement

Industrial Problem and Limitations of Gas Flow Adjustment

A specific industrial problem concerns the tendency to increase shielding gas flow when protection around the

welding region is uncertain. This adjustment may appear straightforward, but its effectiveness depends on the operating conditions. Campbell et al. (2013) identified excessive consumption and undesirable turbulence as potential consequences of high flow rates. They also demonstrated the importance of nozzle geometry and cross-drafts in determining shielding performance. Increasing flow without considering these factors can therefore add cost without resolving the underlying delivery problem.

Existing gas delivery systems allow operators to regulate flow, but a selected flow-meter setting does not independently establish adequate protection or mechanical performance. Beyer et al. (2013) compared conventional flow control with a self-regulating gas-saving device and demonstrated that reduced consumption could maintain weld quality under suitable conditions. However, lower flow rates became more vulnerable to cross-drafts. The manufacturing problem is consequently one of selecting an appropriate operating condition, rather than simply maximising or minimising gas supply(Mamo & Foden, 2013; Suwannatee et al., 2023, p. 1020). This creates a further question for process qualification: when gas flow increases, does the resulting joint exhibit a corresponding mechanical benefit? Answering this question requires measurements relevant to the intended loading condition. Evidence of adequate shielding is important, but it does not, by itself, quantify the load-bearing response of a particular welded specimen.

Critical Synthesis of Previous Research

Previous research has approached shielding gas selection through complementary physical and mechanical assessments. Campbell et al. (2012) found that acceptable weld quality could be maintained at 6 L/min in a draft-free environment. They also associated flow variation with changes in penetration, distortion, and peak temperature. These observations indicate that flow adjustment may affect several aspects of welding performance, although the acceptable setting remains conditional on the surrounding environment. Bitharas et al., (2017) examined these conditions more directly using schlieren imaging, magnetohydrodynamic modelling, and radiographic inspection. Their investigated GMAW configuration achieved sufficient shielding with pure argon at 9 L/min (Chen et al., 2023, p. 6516; Spaniol et al., 2020, p. 877). Whereas flow-control trials assess the practical consequences of changing gas supply, this combined approach provides insight into coverage and interaction with the atmosphere. Nevertheless, successful shielding in that configuration cannot be treated as a transferable flow recommendation for every material, joint, or mechanical loading condition.

Mechanical studies extend the evidence beyond coverage. Pratikno et al. (2022) investigated ASTM A53–A36 joints using pure CO_2 at 15, 20, and 25 L/min with single- and double-V grooves. The highest tensile strength occurred at 25 L/min with a double-V groove. Their findings show why gas flow must be considered alongside joint preparation. However, the preferred combination represents the tested materials and tensile response, rather than a general optimum for GMAW joints. (Malang et al., 2023) examined SPHC steel using currents of 120–140 A and CO_2 flow rates of 15–25 L/min, with tensile and impact properties as response measures. Their factorial investigation incorporated repeated tests, enabling assessment of current, flow rate, and their interaction. This provides a stronger basis for evaluating interacting parameters than an unreplicated comparison. Its conclusions nevertheless concern tensile and impact performance, leaving the compression-test response of the present specimen configuration unresolved. Collectively, these investigations establish that shielding effectiveness, joint preparation, and mechanical loading must inform parameter selection. Their different preferred settings are not necessarily contradictory. They reflect differences in experimental conditions and evaluation criteria. The implication for manufacturing research is that gas flow recommendations require a clearly defined application and response measure.

Mechanical Evaluation and the Specific Research Gap

The present investigation examines welded specimens under compressive loading using a universal testing machine, illustrated in Figure 2. This assessment provides a basis for comparing the maximum recorded loads associated with the selected welding conditions. It also requires careful interpretation: a specimen that bends under an applied compressive load does not necessarily experience uniform uniaxial compression. The recorded load therefore characterises the specimen and loading arrangement, while any calculated stress depends on the reference area and test assumptions.

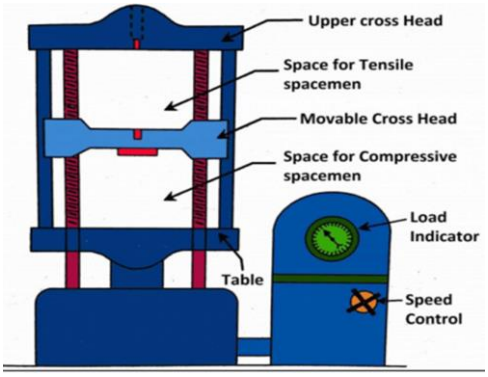


Figure 2. Universal testing machine

Against this background, the research gap concerns the transferability of existing shielding gas evidence to the investigated compression-test configuration. The reviewed studies address gas coverage, flow-control efficiency, tensile properties, or impact resistance. They do not directly establish how flow rates of 10, 20, and 25 L/min relate to the recorded loading response of the present low-carbon steel specimens with a V-groove, dimensions of 100 × 40 × 4 mm, and a welding current of 120 A.

This gap is deliberately bounded. It does not imply that compression behaviour or shielding gas effects have never been studied. Rather, it identifies a specific relationship that the reviewed evidence does not resolve directly. A comparative experiment can provide preliminary observations for this configuration, although establishing reproducibility, statistical significance, or a broadly applicable optimum would require further testing.

Proposed Approach and Research Questions

This study compares the compression-test responses of specimens produced at three shielding gas flow rates: 10, 20, and 25 L/min. The specified welding current, specimen

dimensions, and groove type remain consistent across the comparison. The principal response measure is the maximum recorded load; the corresponding calculated strength values provide an additional comparison subject to verification of the area definition and loading configuration.

The approach differs from the reviewed studies through its focus on a defined compression-test response rather than shielding visualisation, nozzle redesign, or tensile and impact properties. Its purpose is comparative and exploratory. It does not seek to infer unmeasured changes in porosity, microstructure, residual stress, or thermal history. The investigation addresses the following research questions: 1) How does the maximum recorded load differ among specimens welded at shielding gas flow rates of 10, 20, and 25 L/min? 2) Does the specimen welded at 25 L/min exhibit an additional load-bearing benefit relative to the specimen welded at 20 L/min under the investigated conditions? 3) How do the corresponding calculated strength values compare when evaluated using a consistently defined reference area?

Intended Scientific and Technological Contributions

The intended scientific contribution is a clearly bounded comparison connecting shielding gas flow rate with mechanical response under the investigated loading arrangement. This extends the application-specific evidence available for GMAW parameter selection and provides a basis for subsequent experiments using replication, deformation measurements, and weld characterisation. The intended technological contribution is preliminary support for identifying flow settings that merit further procedure qualification. Such evidence may help manufacturers evaluate whether increased gas delivery warrants additional testing for a mechanical benefit. The study does not directly measure production cost, gas savings, or environmental performance, so these outcomes remain outside its demonstrated contribution. What remains unresolved is whether the selected flow settings produce distinguishable and reproducible loading responses in this specimen configuration. By investigating the observed differences without assuming an improvement in advance, the study aims to strengthen the connection between welding parameter selection and mechanical evaluation. Its contribution to manufacturing science lies in providing configuration-specific evidence and defining the conditions under which that evidence can inform further process development.

MATERIALS AND METHODS

Materials, Equipment, and Research Conditions

The investigation used low-carbon steel specimens joined by gas metal arc welding (GMAW). The recorded specimen dimensions were 100 mm in length, 40 mm in width, and 4 mm in thickness. A V-groove configuration and a nominal welding current of 120 A were specified for all three experimental conditions. The material designation, chemical composition, supplier, and certified mechanical properties were not documented sufficiently to establish a specific steel grade. The principal equipment comprised a GMAW welding system, a shielding gas supply, and a universal testing machine for mechanical loading. The welding system and testing machine are illustrated in Figures 1 and 2, respectively. Specimen photographs before and after loading provided supplementary documentation of the observed deformation. The available records do not identify the shielding gas composition or purity, electrode classification and diameter, welding machine model, testing machine capacity, or load measurement accuracy. These specifications are necessary for independent replication and must be established from the original experimental records. The investigation is therefore reported as a preliminary comparison under the documented conditions.

Experimental Design and Specimen Preparation

The study used a single-factor comparative experimental design. Shielding gas flow rate was the experimental factor, with three nominal settings: 10, 20, and 25 L/min. The welding current, groove type, and recorded specimen dimensions were consistent across the three conditions.

Table 1. Experimental conditions used in the comparison

Parameter	Condition G10	Condition G20	Condition G25
Shielding gas flow rate, Q (L/min)	10	20	25
Nominal welding current (A)	120	120	120
Recorded specimen length (mm)	100	100	100
Recorded specimen width (mm)	40	40	40
Recorded specimen thickness (mm)	4	4	4
Groove type	V	V	V
Recorded specimen count	1	1	1

Each specimen was associated with its nominal gas flow setting and subsequently subjected to mechanical loading. The available dataset contains one reported observation per condition. Consequently, the experiment permits comparison among the three recorded specimens but does not provide an estimate of variation within each condition.

Condition G10 served as the internal reference for calculating relative changes. It was not an unwelded control or a reference specimen certified to a testing standard. No additional control group was included in the reported dataset. The records do not specify the groove angle, root gap, root face, surface preparation, welding position, number of passes, or order of specimen production. These preparation details should be supplied before the procedure is presented as independently reproducible.

Process Parameters and Measurement Procedures

The independent variable was the nominal shielding gas flow rate, expressed in L/min. The principal response variable was the maximum recorded load, $F_{\max}$, expressed in kilogram-force (kgf). A secondary response was the load-normalized value calculated using the reference area adopted in the original analysis. The documented comparison variables were welding current, specimen dimensions, and groove type. Other potentially influential parameters, including arc voltage, wire feed speed, travel speed, contact-tip-to-work distance, torch angle, and interpass temperature, were not sufficiently documented to confirm equivalent operating conditions. Following welding, each specimen underwent loading in the universal testing machine. The reported maximum load was retained as the primary mechanical observation. Photographs taken before and after testing documented the specimen condition and bending deformation. These photographs support

qualitative description but do not independently quantify strain, displacement, or fracture characteristics.

The available records do not specify the loading direction relative to the weld, support spacing, contact geometry, loading rate, preload, displacement measurement, data acquisition frequency, or stopping criterion. No specific mechanical testing standard can therefore be claimed as having been followed. Because bending occurred during loading, the recorded response should be interpreted in relation to the test configuration rather than assumed to represent uniform uniaxial compression. Calibration certificates, instrument resolution, and measurement uncertainty were not available in the supplied records. Accordingly, no numerical uncertainty bounds were assigned.

Analytical Procedures and Definition of Response Measures

The analysis compared maximum recorded loads and reproduced the calculations underlying the reported Results. No computational model, optimisation algorithm, or mechanistic simulation was used. For consistency with the original calculation, the reference area was defined as:

$$A_{ref} = 2(P_0L_0 + P_0T_0 + L_0T_0) \quad (1)$$

where \(P_0\), \(L_0\), and \(T_0\) denote the recorded specimen length, width, and thickness, respectively, in millimetres. Substituting the documented dimensions gives:

$$A_{ref} = 2[(100 \times 40) + (100 \times 4) + (40 \times 4)] = 9120\ mm^2$$

Equation (1) calculates the total external surface area of a rectangular prism. It does not calculate the cross-sectional area perpendicular to the applied load. The corresponding quantity is therefore designated here as a **load-normalized index**, I_L, rather than an intrinsic material compressive strength:

$$I_L = \frac{F_{max}}{A_{ref}} \quad (2)$$

where I_L is expressed in kgf/mm² when F max is expressed in kgf.

This definition preserves the numerical basis of the existing Results while distinguishing the reported calculation from a validated compressive stress measurement. Calculation of engineering compressive stress would instead require a verified load-bearing cross-sectional area and an appropriate loading configuration. Where force conversion was required, kilogram-force was converted to newtons using:

$$F_{max,N} = 9.80665 \times F_{max,kgf} \quad (3)$$

Conversion of the index to N/mm² changes its units but does not resolve the geometric limitation of the reference area.

Performance Evaluation and Experimental Limitations

Performance evaluation used the maximum recorded load as the primary comparison metric. The load-normalized index provided a secondary metric consistent with the original numerical analysis. Because all specimens used the same reference area, the index preserves the ranking of the recorded loads and does not constitute an independent mechanical measurement. Relative differences between conditions were calculated as:

$$\Delta F_{a\to b} = \left(\frac{F_{max,b} - F_{max,a}}{F_{max,a}}\right) \times 100\% \quad (4)$$

where a and b represent the conditions being compared.

The evaluation considered the changes from 10 to 20 L/min, from 20 to 25 L/min, and from the reference condition to each higher-flow condition. These comparisons describe the recorded observations. They do not establish statistical significance, repeatability, or a generally applicable optimum. No replicated trials, independently measured reference properties, or separate validation dataset were available. Process variability and measurement uncertainty could therefore not be separated from differences associated with gas flow setting. Likewise, an equal reported response at two settings cannot establish equivalence without repeated measurements and a defined equivalence criterion.

Data Analysis and Reproducibility

The analysis used the three recorded maximum loads, the nominal process settings, and the documented specimen dimensions. All observations were retained. No values were imputed, and no outliers were removed. Data processing comprised checking units, reproducing the reference-area calculation, calculating the load-normalized index, and determining relative differences using unrounded values. Rounding was applied only when presenting the final numerical values. The flow-rate comparison used a numerical horizontal axis so that the spacing between 10, 20, and 25 L/min represented the actual differences between settings. No inferential statistical tests were performed because the dataset contained one observation per condition. Standard deviations, confidence intervals, and significance thresholds were therefore not reported. The software and version used for the original analysis were not documented; the equations above specify the arithmetic required to reproduce the calculations.

Potential sources of bias include undocumented welding parameters, specimen preparation differences, loading alignment, and the absence of randomised production and testing orders. These limitations restrict interpretation to the recorded specimens. Reproducibility requires preservation of the original load records, specimen identification, dimensional measurements, photographs, equipment specifications, and completed welding and testing procedures.

RESULTS

The strength of the welded pipe joints was calculated to determine the reported compressive strength associated with bending deformation.

$$KT = \frac{F'_{max}}{A_0}$$

Equation key: KT = compressive strength (kgf/mm²); Fmax = maximum load (kgf); Ao = initial cross-sectional area (mm²). Table 1 presents the specimen parameters before testing.

Table 1. Test specimen parameters

No.	Specimen	P_0 (mm)	L_0 (mm)	T_0 (mm)	A_0 (mm²)	Groove Type	Welding Current (A)	Fmax (kgf)
1	Shielding gas flow rate of 10 L/min	100	40	4	9,120	V	120	440
2	Shielding gas flow rate of 20 L/min	100	40	4	9,120	V	120	460
3	Shielding gas flow rate of 25 L/min	100	40	4	9,120	V	120	460

Image table key: No = number; Spesimen = specimen; Laju gas = gas flow rate; Kampuh = groove; Arus = current; liter/mnt = L/min. Po, Lo, To, Ao, and Fmax are defined below Table 2. All numerical entries are retained from the original image.

Specimen welded at a shielding gas flow rate of 10 L/min



Figure 3. Specimen welded at 10 L/min before and after testing

A. Calculation of the initial cross-sectional area

Ao = 2 × ((Po × Lo) + (Po × To) + (Lo × To)) = 9,120 mm²

B. Calculation of specimen compressive strength

$$KT = \frac{F'_{max}}{A_0}$$

= 0.048 kgf/mm²

Specimen welded at a shielding gas flow rate of 20 L/min



Figure 4. Specimen welded at 20 L/min before and after testing

A. Calculation of the initial cross-sectional area

Ao = 2 × ((Po × Lo) + (Po × To) + (Lo × To)) = 9,120 mm²

KT = 0.050 kgf/mm²

Specimen welded at a shielding gas flow rate of 25 L/min.



Figure 5. Specimen welded at 25 L/min before and after testing

A. Calculation of the initial cross-sectional area

Ao = 2 × ((Po × Lo) + (Po × To) + (Lo × To))

= 9,120 mm²

B. Calculation of specimen compressive strength

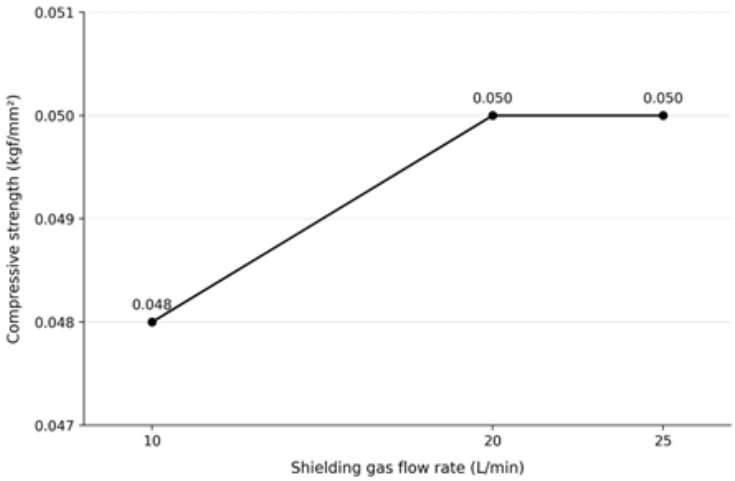
$$KT = \frac{F'_{max}}{A_0}$$

= 0.050 kgf/mm²

Table 2. Calculated results for the shielding gas flow rates

No.	Specimen	Po (mm)	Lo (mm)	To (mm)	Ao (mm²)	Groove	I (A)	Fmax (kgf)	KT (kgf/mm²)
1	Gas flow 10 L/min	100	40	4	9,120	V	120	440	0.048
2	Gas flow 20 L/min	100	40	4	9,120	460	0.050		
3	Gas flow 25 L/min	100	40	4	9,120	460	0.050		

where: Po = initial length (mm); Lo = initial width (mm); To = initial thickness (mm); Ao = initial cross-sectional area (mm²); Fmax = maximum load (kgf); KT = compressive strength (kgf/mm²).



Note. Original graph label key: Kuat Tekan = compressive strength (kgf/mm²); Laju Gas Pelindung = shielding gas flow rate (L/min).

Figure 6. Compressive strength versus shielding gas flow rate.

Figure 6 presents the compression test results for pipe joints welded at shielding gas flow rates of 10, 20, and 25 L/min. The specimen welded at 10 L/min exhibited a reported compressive strength of 0.048 kgf/mm². The specimens welded at 20 and 25 L/min each exhibited a reported compressive strength of 0.050 kgf/mm².

DISCUSSION

Principal Findings and Their Scientific Interpretation

The principal finding is a difference in the maximum recorded load between the specimen welded at 10 L/min and those welded at 20 and 25 L/min. The latter two specimens exhibited the same reported maximum load. Within the available dataset, increasing shielding gas flow was therefore associated with an improvement between the first two settings, followed by no additional recorded benefit at the highest setting. This pattern qualifies the assumption that increasing gas flow necessarily produces a continuous

improvement in mechanical performance. A plausible explanation for this plateau is that, beyond a certain flow rate, additional shielding gas no longer changes the effective protection of the weld pool, so that other factors such as heat input and joint geometry govern the observed load capacity.

The interpretation should focus primarily on maximum recorded load. The calculated values presented as compressive strength were obtained by dividing the load by the total external surface area of a rectangular specimen(Jiang et al., 2018, p. 251; Tita-Goldstein, 2013, p. 61). This denominator does not represent the cross-sectional area perpendicular to the applied load(Cruz et al., 2022, p. 8; Dhoska et al., 2018, p. 13). Consequently, these values describe the load-normalized index defined in the revised Methods rather than an independently established material compressive strength. Because the same reference area was used for every specimen, the index reproduces the load ranking without providing additional evidence about intrinsic material properties.

The recorded increase from 440 to 460 kgf corresponds to approximately 4.55% when calculated from the reported loads. However, this difference cannot be interpreted as a statistically established treatment effect. With one reported observation per condition and no quantified measurement uncertainty, the experiment cannot distinguish a reproducible gas-flow effect from specimen variability or differences in welding and testing conditions.

Comparison with Previous Research

The observed response is consistent with the broader understanding that shielding gas requirements depend on the welding configuration. Campbell et al. (2012) maintained acceptable weld quality at reduced flow rates under draft-free conditions but identified increased sensitivity to cross-drafts. Bitharas et al. (2017) likewise demonstrated sufficient coverage at relatively low flow in their investigated GMAW configuration. These studies indicate that additional gas delivery does not automatically produce additional quality benefits. Nevertheless, their coverage and weld-quality assessments cannot directly validate the present mechanical observations because their materials, delivery conditions, and evaluation criteria differ. Accordingly, the present study does not establish whether the observed plateau between 20 and 25 L/min reflects a general saturation of shielding performance, and this question should be addressed through replicated measurements under controlled stand-off distances and gas delivery conditions. Such replication would also clarify whether the reference-area normalization used here alters the apparent ranking, since a true cross-sectional basis may respond differently to changes in weld bead geometry and porosity, as the stand-off study showed that weld seam porosity was unaffected across the tested range while shield gas flow rate remained the controlling parameter(Coroado et al., 2017, p. 3171; Wordofa & Ramulu, 2023, p. 370) . The closest mechanical comparison is the investigation by Pratikno et al. (2022), who examined ASTM A53–A36 joints at 15, 20, and 25 L/min using different V-groove configurations. Their highest tensile strength occurred at 25 L/min with a double-V groove. The present absence of an additional recorded load benefit between 20 and 25 L/min does not contradict that finding. Their study evaluated tensile performance in a different material and joint configuration(Elfallah, 2022, p. 18703). Together, the investigations indicate that a preferred flow setting must be linked to the specific response being evaluated rather than transferred directly between applications. Malang et al. (2023) investigated current and gas-flow combinations through replicated tensile and impact testing of SPHC steel. Their experimental design addressed interactions between parameters, whereas the present dataset supports only a descriptive comparison across flow settings at a specified current. Their findings reinforce the relevance of gas flow to mechanical evaluation, but also illustrate why replication and control of interacting parameters are necessary before a preferred setting can be established with confidence.

Plausible Process Relationships and Mechanistic Explanations

One possible explanation for the lower recorded load at 10 L/min is that shielding conditions differed sufficiently to influence joint formation. Bitharas et al. (2017) showed that gas coverage depends on interactions among the shielding stream, arc, nozzle position, and atmosphere. If coverage at the lowest setting was inadequate in the present arrangement, differences in weld integrity could have contributed to the observed response. However, the study did not measure coverage, oxygen concentration, or internal discontinuities.(Egerland et al., 2018, p. 847; Silva et al., 2021, p. 48). Insufficient shielding therefore remains a hypothesis rather than an experimentally demonstrated cause. Consistent with this interpretation, the broader literature suggests that shielding failure at low flow is more likely to manifest as porosity and reduced weld soundness than as a uniform change in strength, which would make the observed difference in maximum load a secondary indicator rather than a direct measure of coverage(Reijonen et al., 2020; Silvério et al., 2021, p. 10) .

A second possibility concerns changes in thermal behaviour and weld geometry. Campbell et al. (2012) associated gas-flow variation with penetration, distortion, and peak temperature. Such relationships provide a technical basis for investigating whether gas delivery affected the geometry or mechanical response of the present joints. The available photographs alone cannot establish these mechanisms, because penetration depth, weld dimensions, temperature history, and residual stresses were not quantified(Drexler et al., 2019, p. 14; Hu et al., 2022, p. 5821). Consequently, the mechanistic interpretations offered above should be regarded as testable hypotheses, and their confirmation would require measurement of penetration profiles, porosity distribution, and fracture surface characteristics across replicated specimens at each flow setting.

The equal maximum loads at 20 and 25 L/min could indicate that additional flow provided no measurable benefit under the tested conditions. They could also reflect limited instrument resolution, rounding, or specimen differences. Although excessive flow can introduce turbulence, as discussed by Campbell et al. (2013), the present observations do not demonstrate that turbulence occurred at 25 L/min. No reduction in recorded load was observed at that setting, and gas-flow behaviour was not measured.

Contribution to Manufacturing Science and Conditions of Applicability

The study provides a preliminary connection between shielding gas setting and the loading response of a defined welded-specimen configuration. Its contribution is the

compression-test comparison at a specified current, groove type, and recorded specimen size. It extends the application-specific discussion of shielding gas selection beyond the tensile, impact, and coverage responses considered in the reviewed investigations.

The comparison also highlights the importance of selecting an appropriate performance indicator. A maximum load characterises the tested specimen and loading arrangement. An intrinsic material strength requires an appropriate stress definition and test configuration. Maintaining this distinction improves the connection between manufacturing parameters, mechanical measurements, and the conclusions drawn from them.

Within the reported tests, the specimens welded at 20 and 25 L/min performed better in terms of maximum recorded load than the specimen welded at 10 L/min. This observation is insufficient to classify any setting as universally satisfactory or unsuitable. No acceptance threshold, unwelded baseline, or qualified reference procedure was provided. The findings apply only to the recorded specimens and cannot establish performance under different gas compositions, nozzle arrangements, welding currents, material grades, or service loads.

Practical Implications for Process Selection and Resource Use

The practical implication is that 20 L/min merits further evaluation because the specimen produced at this setting reached the same reported maximum load as the specimen produced at 25 L/min. A manufacturer could use this observation to define a subsequent qualification experiment, rather than adopt 20 L/min immediately as an optimum.

A lower flow setting could reduce shielding gas use if welding duration and other operating conditions remained unchanged. This is a projected benefit, not a demonstrated outcome of the present study. Actual gas consumption, leakage, pre-flow, post-flow, and welding duration were not measured(Society et al., 2022, p. 241, 2023, p. 134). Financial savings therefore cannot be quantified from the available results. Any future assessment of gas economy should therefore be designed to record consumption directly, so that the relationship between flow setting, shielding performance, and operating cost can be established experimentally rather than inferred.

The study likewise provides no direct evidence of improved productivity, reduced energy consumption, lower emissions, or reduced material waste. Those outcomes would require measurements such as cycle time, electrical energy, gas consumption, rejection rate, and rework frequency. The experimentally supported statement is narrower: additional nominal gas flow from 20 to 25 L/min produced no additional reported maximum-load benefit in the available observations.

Robustness, Generalizability, and Threats to Validity

The principal limitation is the absence of documented replication. A single observation per setting does not permit estimation of within-condition variability, confidence intervals, or statistical significance. It also prevents an equivalence conclusion for the two higher-flow conditions. Equal reported values are not sufficient to establish that their underlying performance distributions are equivalent.

Internal validity is further limited by incomplete documentation of gas composition, electrode characteristics, arc voltage, travel speed, torch position, and specimen preparation(Evans et al., 2022, p. 1519; Martina et al., 2012, p. 1378). Although current, dimensions, and groove type were nominally consistent, other influential conditions were not verified. Differences in these factors could contribute to the measured response and weaken causal attribution to gas flow.

Measurement validity remains affected by the unspecified loading configuration, observed bending, and reference-area calculation. The absence of calibration and uncertainty information makes it impossible to determine whether the recorded difference exceeds the combined variability of the measurement and preparation procedures. The tests also do not establish pipe pressure resistance, fatigue performance, or structural service reliability.

Generalizability is consequently limited. The observations support a local comparison and a basis for further investigation. Broader recommendations require independently prepared replicate specimens, documented welding procedures, verified loading geometry, calibrated instrumentation, and an appropriate mechanical testing protocol.

Relationship to Existing Knowledge and Further Research

The findings qualify the proposition that increasing shielding gas flow continuously improves welded-joint performance. They are compatible with previous evidence that suitable flow settings depend on the process configuration, but they do not establish the physical mechanism responsible for the recorded differences. Future work should therefore combine replicated welds with arc observation, shielding-gas coverage measurements, and fracture-surface analysis, so that any proposed mechanism can be tested rather than assumed, as recommended in the broader literature on weld-quality assessment (Prasetyo et al., 2023, p. 73). Such an approach would also allow the influence of gas flow to be separated from the effects of arc behaviour and filler-material variability, which the reviewed studies have shown can dominate the scatter in measured strength (Fortan et al., 2020, p. 106104; Schilling et al., 2026, p. 3477). Such a combined design would also clarify whether the observed sensitivity to flow setting is consistent across welding conditions, since the reviewed evidence indicates that factors such as current, voltage and gas flow interact in determining joint response rather than acting independently (Boris, 2026, p. 22). Further work should prioritise repeatability and measurement validity before expanding the parameter range. Replicated tests with verified geometry would establish whether the load difference persists. Weld cross-sections, radiographic inspection, and dimensional measurements could then examine whether coverage, penetration, or discontinuities explain the response. Such evidence would allow the present descriptive comparison to develop into a stronger process–structure–performance investigation. Such an investigation would also benefit from documenting the complete welding procedure, including gas composition, electrode geometry, arc voltage, and travel speed, so that the contribution of shielding gas flow can be isolated from other influential variables (Muddin et al., 2024, p. 29). Such an approach would also make it possible to determine whether the reported load differences are reproducible under documented loading geometry and calibrated measurement

conditions, rather than reflecting unrecorded procedural variation (Kareem et al., 2023, p. 126). The present study therefore offers preliminary evidence for targeted process qualification. Its manufacturing value lies in identifying a question for controlled testing: whether the lower of the two higher-flow settings can maintain reproducible joint performance without unnecessary gas delivery.

CONCLUSION

This study compared the compression-test responses of low-carbon steel GMAW specimens produced at shielding gas flow rates of 10, 20, and 25 L/min. The maximum recorded load increased from 440 kgf at 10 L/min to 460 kgf at 20 L/min, a descriptive increase of 4.55%. The specimen welded at 25 L/min also reached 460 kgf, indicating no additional recorded load benefit over 20 L/min.

The study contributes preliminary, configuration-specific evidence linking shielding gas settings with mechanical loading response. The observations identify 20 L/min as a candidate for further procedure qualification, but do not establish an optimum or demonstrate gas savings. The calculated load-normalized values should not be interpreted as intrinsic compressive strength because the reference area represents specimen surface area rather than the load-bearing cross-section.

The findings remain limited by one reported observation per condition, incomplete process documentation, and unquantified measurement uncertainty. Future research should use independently prepared replicate specimens, a verified loading configuration, and calibrated load and displacement measurements to determine whether the observed difference is reproducible.

DECLARATIONS

Acknowledgements

The authors thank Politeknik Teknologi Kimia Industri Medan and the Faculty of Engineering, Universitas Muhammadiyah Sumatera Utara, Indonesia, for their academic and institutional support throughout this study.

Funding

This research received no specific grant from funding agencies in the public, commercial, or not-for-profit sectors.

Declaration of Competing Interests

The authors declare that they have no known competing financial interests or personal relationships that could have influenced the work reported in this paper.

CRediT Author Contributions

Manahan Hutagallung: Conceptualization, Methodology, Investigation, Formal analysis, Writing – original draft.

Ricky Sanjaya: Investigation, Data curation, Visualization, Writing – review & editing.

Data Availability Statement

The available numerical data supporting the findings are included in the article. Additional raw measurement records are not available.

Code and Software Availability

The equations and calculation procedures used for the numerical analysis are described in the Materials and Methods section.

REFERENCES

Beyer, V., Campbell, S. W., Ramsey, G., Galloway, A., Moore, A. J., & McPherson, N. A. (2013). Systematic study of effect of cross-drafts and nozzle diameter on shield gas coverage in MIG welding. *Science and Technology of Welding & Joining*, *18*(8), 652–660. https://doi.org/10.1179/1362171813y.0000000143

Bitharas, I., McPherson, N. A., McGhie, W., Roy, D., & Moore, A. J. (2017). Visualisation and optimisation of shielding gas coverage during gas metal arc welding. *Journal of Materials Processing Technology*, *255*, 451–462. https://doi.org/10.1016/j.jmatprotec.2017.11.048

Boris, N. (2026). Optimization of Tungsten Inert Gas Welding Process on the Tensile Properties of Dissimilar Metal Using Taguchi Method. *Advances in Materials*, *15*(1), 14–26. https://doi.org/10.11648/j.am.20261501.12

Campbell, S. W., Galloway, A., & McPherson, N. A. (2012). Techno-economic evaluation of reducing shielding gas consumption in GMAW whilst maintaining weld quality. *The International Journal of Advanced Manufacturing Technology*, *63*, 975–985. https://doi.org/10.1007/s00170-012-3961-2

Campbell, S. W., Galloway, A., & McPherson, N. A. (2013). Gmaw Shielding Gas Flow Optimisation by Refinement of Nozzle Geometry. In *Springer eBooks* (pp. 2131–2137). Springer Nature. https://doi.org/10.1007/978-3-319-48764-9_265

Chen, A., Li, B., Chen, X., Jiang, M., Zou, S., Tao, W., Lei, Z., & Chen, Y. (2023). Experimental and Numerical Investigation of Shielding Gas Behaviors in Laser Welding of TC4 Alloy. *Materials*, *16*(19), 6511. https://doi.org/10.3390/ma16196511

Coroado, J., Meco, S., Williams, S., Ganguly, S., Suder, W., Quintino, L., & Assunção, E. (2017). Fundamental understanding of the interaction of continuous wave laser with aluminium. *The International Journal of Advanced Manufacturing Technology*, *93*, 3165–3174. https://doi.org/10.1007/s00170-017-0702-6

Cruz, E. N. S., Vélez, A. M., Mendoza, E. A. O., & Guillén, C. A. G. (2022). Compressive Strength Test of Interlocked Blocks Made with High-Mechanical-Performance Mortars. In *IntechOpen eBooks*. IntechOpen. https://doi.org/10.5772/intechopen.107174

Dhoska, K., Tola, S., Pramono, A., & Vozga, I. (2018). Evaluation of measurement uncertainty for the determination of the mechanical resistance of the brick samples by using uniaxial compressive strength test. *International Journal of Metrology and Quality Engineering*, *9*, 12. https://doi.org/10.1051/ijmqe/2018012

Drexler, E. S., Slifka, A. J., Amaro, R. L., Sowards, J. W., Connolly, M., Martin, M. L., & Lauria, D. S. (2019). Fatigue Testing of Pipeline Welds and Heat-Affected Zones in Pressurized Hydrogen Gas. *Journal of Research of the National Institute of Standards and Technology*, *124*, 1–19. https://doi.org/10.6028/jres.124.008

Egerland, S., Colegrove, P. A., & Williams, S. (2018). Arc instabilities during split anode calorimetry with the TIG welding process. *Welding in the World*, *62*(4), 831–845. https://doi.org/10.1007/s40194-018-0588-4

Elfallah, S. S. S. (2022). Study on the influence of groove shape on the tensile strength of commercial steel. *Journal of Engineering Research*, *11*(3), 18695. https://doi.org/10.36909/jer.18695

Evans, S., Wang, J., Qin, J., He, Y., Shepherd, P., & Ding, J. (2022). A review of WAAM for steel construction – Manufacturing, material and geometric properties, design, and

future directions. *Structures*, *44*, 1506–1522. https://doi.org/10.1016/j.istruc.2022.08.084

Fortain, J. M., & Gadrey, S. (2013). How to select a suitable shielding gas to improve the performance of MIG and TIG welding of aluminium alloys. *Welding International*, *27*(12), 936–947. https://doi.org/10.1080/09507116.2012.753257

Fortan, M., Dejans, A., Karabulut, B., Debruyne, D., & Rossi, B. (2020). On the strength of stainless steel fillet welds. *Journal of Constructional Steel Research*, *170*, 106081. https://doi.org/10.1016/j.jcsr.2020.106081

Hu, Y., Wu, S., Guo, Y., Shen, Z., Korsunsky, A. M., Yu, Y., Zhang, X., Fu, Y., Che, Z., Xiao, T., Lozano-Perez, S., Yuan, Q., Zhong, X., Zeng, X., Kang, G., & Withers, P. J. (2022). Inhibiting weld cracking in high-strength aluminium alloys. *Nature Communications*, *13*(1), 5816. https://doi.org/10.1038/s41467-022-33188-x

Jia, C., Li, W., Sun, G., Zhang, M., Meng, Y., Liu, J., & Chen, C. (2025). Variations and mechanisms in the Ti6Al4V alloy MIG welding process under coaxial dual-path shielding gas-flow field. *Journal of Materials Research and Technology*, *39*, 9083–9106. https://doi.org/10.1016/j.jmrt.2025.11.222

Jiang, J., Zhang, J., Liu, J., Chiew, S. P., & Lee, C. K. (2018). Effect of welding and heat treatment on strength of high-strength steel columns. *Journal of Constructional Steel Research*, *151*, 238–252. https://doi.org/10.1016/j.jcsr.2018.09.027

Kareem, S. S. A. A., Mahdi, B. L., & Hussein, H. K. (2023). Impact of TIG Welding Parameters on the Mechanical Properties of 6061-T6 Aluminum Alloy Joints. *Advances in Science and Technology – Research Journal*, *17*(5), 114–129. https://doi.org/10.12913/22998624/171489

Liu, G., Tang, X., Xu, Q., Lu, F., & Cui, H. (2021). Effects of Active Gases on Droplet Transfer and Weld Morphology in Pulsed-Current NG-GMAW of Mild Steel. *Chinese Journal of Mechanical Engineering*, *34*(1). https://doi.org/10.1186/s10033-021-00583-2

Malang, P. N., Amrullah, R. N., Subagiyo, S., & Malang, P. N. (2023). Effect of Current Strength and Flow Rate of Shielding Gas on the Impact and Tensile Strength of GMAW Welsing Result on SPHC Materials. *Logic Jurnal Rancang Bangun Dan Teknologi*, *23*(3), 194–202. https://doi.org/10.31940/logic.v23i3.194-202

Mamo, S., & Foden, J. (2013). Understanding the shielding gas dynamics and improving the weld quality in MIG/MAG welding with respect to draughts. *Zavarivanje i Zavarene Konstrukcije*, *58*(2), 61–80. https://scindeks-clanci.ceon.rs/data/pdf/0354-7965/2013/0354-79651302061M.pdf

Martina, F., Mehnen, J., Williams, S., Colegrove, P. A., & Wang, F. (2012). Investigation of the benefits of plasma deposition for the additive layer manufacture of Ti–6Al–4V. *Journal of Materials Processing Technology*, *212*(6), 1377–1386. https://doi.org/10.1016/j.jmatprotec.2012.02.002

Muddin, S., Ariyanto, A., Sriwati, S., & Rahman, M. F. (2024). Optimization of welding direction model parameters to enhance the tensile strength of ST 42 steel joints through variation of current strength simulation. *Eastern-European Journal of Enterprise Technologies*, *2*, 23–31. https://doi.org/10.15587/1729-4061.2024.295536

Prasetyo, E., Baskoro, A. S., Widyianto, A., & Kiswanto, G. (2023). Identifying the influence of orbital pipe welding parameters on mechanical properties using SS316L pipe. *Eastern-European Journal of Enterprise Technologies*, *5*, 72–84. https://doi.org/10.15587/1729-4061.2023.287397

Pratikno, H., Dhanistha, W. L., & Samiyono, A. N. (2022). Analyzing the Effect of Variation in Shielding Gas Flow Rate and V Groove Type Towards Tensile and Metallographic Testing of GMAW Weld Joint of ASTM A53 and A36. *International Journal of Offshore and Coastal Engineeing*, *4*(1), 35–41. https://doi.org/10.12962/j2580-0914.v4i1.8706

Reijonen, J., Revuelta, A., Riipinen, T., Ruusuvuori, K., & Puukko, P. (2020). On the effect of shielding gas flow on porosity and melt pool geometry in laser powder bed fusion additive manufacturing. *Additive Manufacturing*, *32*, 101030. https://doi.org/10.1016/j.addma.2019.101030

Schilling, P., Ungethüm, T., Sanderbrand, P., & Schmale, H. C. (2026). Investigation of a multi-cathode TIG arc process for additive manufacturing applications. *Welding in the World*, *70*(8), 3473–3484. https://doi.org/10.1007/s40194-026-02414-1

Silva, L. J. da, Teixeira, F. R., Araújo, D. B. de, Reis, R. P., & Scotti, A. (2021). Work Envelope Expansion and Parametric Optimization in WAAM with Relative Density and Surface Aspect as Quality Constraints: The Case of Al5Mg Thin Walls with Active Cooling. *Journal of Manufacturing and Materials Processing*, *5*(2), 40. https://doi.org/10.3390/jmmp5020040

Silvério, M. G. de C., Raposo, L. H. A., Lopes, R. T., & Júnior, P. C. S. (2021). Evaluation of X-shaped welded joints with Co-Cr alloy under different welding parameters: analysis by micro-CT and flexural strength. *Research Society and Development*, *10*(4). https://doi.org/10.33448/rsd-v10i4.14308

Society, A. W., Cheepu, M., BAEK, H. J., KIM, Y. S., & CHO, S. M. (2022). Penetration Estimation of GTAW with C-Type Filler by Net Heat Input Ratio. *Welding Journal*, *101*(9), 240–248. https://doi.org/10.29391/2022.101.018

Society, A. W., HANSEN, J., & Harwig, D. (2023). Impact of Electrode Rotation on Aluminum GMAW Bead Shape. *Welding Journal*, *102*(6), 125–136. https://doi.org/10.29391/2023.102.010

Spaniol, E., Trautmann, M., Ungethüm, T., Hertel, M., Füssel, U., Henckell, P., & Bergmann, J. P. (2020). Development of a highly productive GMAW hot wire process using a two-dimensional arc deflection. *Welding in the World*, *64*(5), 873–883. https://doi.org/10.1007/s40194-020-00880-9

Suwannatee, N., Yamamoto, M., & SHINOHARA, S. (2023). Optimization of hot-wire fraction for enhance quality in GMAW. *Welding in the World*, *68*(5), 1017–1032. https://doi.org/10.1007/s40194-023-01623-2

Tita-Goldstein, A. (2013). Particle design by compaction : Influence of process and formulation parameters on end-use properties. *HAL (Le Centre Pour La Communication Scientifique Directe)*. https://hal.univ-lorraine.fr/tel-01750532

Wordofa, T. N., & Ramulu, P. J. (2023). Gas Metal Arc Welding Input Parameters Impacts on Weld Quality Characteristics of Steel Materials a Comprehensive Exploration. *Manufacturing Technology*, *23*(3), 366–379. https://doi.org/10.21062/mft.2023.046